ARTICLE

doi:10.1038/nature11417

# Small heat-shock proteins protect from heat-stroke-associated neurodegeneration

Nikos Kourtis[1], Vassiliki Nikoletopoulou[1] & Nektarios Tavernarakis[1]

**Heat stroke is a life-threatening condition, characterized by catastrophic collapse of thermoregulation and extreme hyperthermia. In recent years, intensification of heat waves has caused a surge of heat-stroke fatalities. The mechanisms underlying heat-related pathology are poorly understood. Here we show that heat stroke triggers pervasive necrotic cell death and neurodegeneration in *Caenorhabditis elegans*. Preconditioning of animals at a mildly elevated temperature strongly protects from heat-induced necrosis. The heat-shock transcription factor HSF-1 and the small heat-shock protein HSP-16.1 mediate cytoprotection by preconditioning. HSP-16.1 localizes to the Golgi, where it functions with the $Ca^{2+}$- and $Mn^{2+}$-transporting ATPase PMR-1 to maintain $Ca^{2+}$ homeostasis under heat stroke. Preconditioning also suppresses cell death inflicted by diverse insults, and protects mammalian neurons from heat cytotoxicity. These findings reveal an evolutionarily conserved mechanism that defends against diverse necrotic stimuli, and may be relevant to heat stroke and other pathological conditions involving necrosis in humans.**

Heat-related pathologies such as heat stroke are estimated to soon become one of most serious causes of mortality[1]. Climatic shifts and other contemporary anthropogenic causes contribute to raise prevalence of hyperthermia incidents and associated deaths[2]. During heat stroke, core body temperature in excess of 40 °C elicits acute tissue injury and multi-organ failure that is often fatal[3]. The nervous system is particularly vulnerable. Heat-stroke survivors commonly suffer permanent neurological damage[4]. The devastating impact of hyperthermia on human health is a consequence of immediate effects of heat on cellular and organismal physiology, coupled with secondary inflammatory and coagulation responses[5]. Despite the severity and increasingly prevalent health risks associated with heat-inflicted damage, the cellular and molecular mechanisms responsible for the direct cytotoxicity of heat are not understood well.

## Heat stroke kills by inducing necrosis

To gain insight into the molecular basis of heat cytotoxicity and to circumvent the confounding influence of secondary physiological and inflammatory responses, we developed and characterized a genetically tractable model of heat stroke in *C. elegans*, a poikilothermic, nematode worm that normally grows at ambient temperature. *C. elegans* is particularly suitable for investigating the direct cytotoxicity of heat because it lacks elaborate thermal regulation systems that would offset elevated external temperature by mounting homeothermic responses. Worms instantly equilibrate to ambient temperature. To simulate hyperthermia, we exposed synchronous nematode populations to 39 °C for 15 min. We then assessed animal survival 16 to 18 h after delivery of the noxious heat pulse (Supplementary Fig. 1a). Excessive heat caused immediate changes in animal behaviour and marked increase of mortality. Ultimately, less than 25% of animals survived heat stroke (Fig. 1a).

We observed widespread cell death in several tissues of afflicted individuals (Fig. 1b, c and Supplementary Fig. 2). Dying cells showed necrotic morphological features (Supplementary Fig. 1c and Supplementary Fig. 3a–e), expressed markers of necrotic death[6] (Supplementary Fig. 1d), and became permeable to propidium iodide (Supplementary Fig. 1e). Loss of key apoptosis or autophagy mediators did not suppress heat-stroke-induced mortality (Supplementary Fig. 4a, b). Moreover, autophagy was not upregulated in animals exposed to heat stroke (Supplementary Fig. 4c, d). Therefore, cell death consequent to heat stroke does not depend on the core apoptotic or autophagic machinery. In contrast, depletion of proteins required for necrosis[6,7] strongly promotes survival after heat stroke (Supplementary Fig. 4e). Thus, we conclude that heat stroke compromises viability by triggering extensive necrotic cell death in the nematode.

## Preconditioning defends against hyperthermia

All organisms possess homeostatic mechanisms that promote survival by mounting adaptive responses to stressors[8]. Acute insults such as extreme heat may cause necrosis by overwhelming cellular homeostasis. Interestingly, pre-exposure to mild stress often elicits increased resistance to subsequent severe stress, a phenomenon termed hormesis[9]. We investigated whether experiencing intermediate, non-lethal temperature before heat stroke (preconditioning) evokes a similar hormetic effect in *C. elegans*. We found that preconditioning at 34 °C for 30 min (Supplementary Fig. 1a) markedly enhanced the capacity of animals to withstand heat stroke (Fig. 1a and Supplementary Figs 1c and 2). Survivors maintained viability over several days after heat stroke and showed no behavioural defects compared to untreated controls (Supplementary Fig. 5 and Supplementary Table 1).

Preconditioning may exert its protective effect by engaging the heat-shock-response pathway to fortify cells under extreme temperature. To test this idea, we examined mutants lacking HSF-1, the transcription factor that coordinates the heat-shock response[10]. Preconditioning does not increase survival of these animals, indicating that HSF-1 is required for protection against heat stroke. Moreover, overexpression of HSF-1 suppresses necrotic cell death and augments survival further, both after and without preconditioning (Fig. 1a and Supplementary Fig. 2). Therefore, HSF-1 is necessary and sufficient to render animals resistant to heat stroke.

Low insulin-like signalling (ILS) increases intrinsic thermotolerance of *C. elegans* during prolonged incubation at intermediate temperature (35 °C)[11]. We find that ILS deficiency enhances survival after heat stroke, both with and without preconditioning (Supplementary

[1]Institute of Molecular Biology and Biotechnology, Foundation for Research and Technology, Heraklion 71110, Crete, Greece.

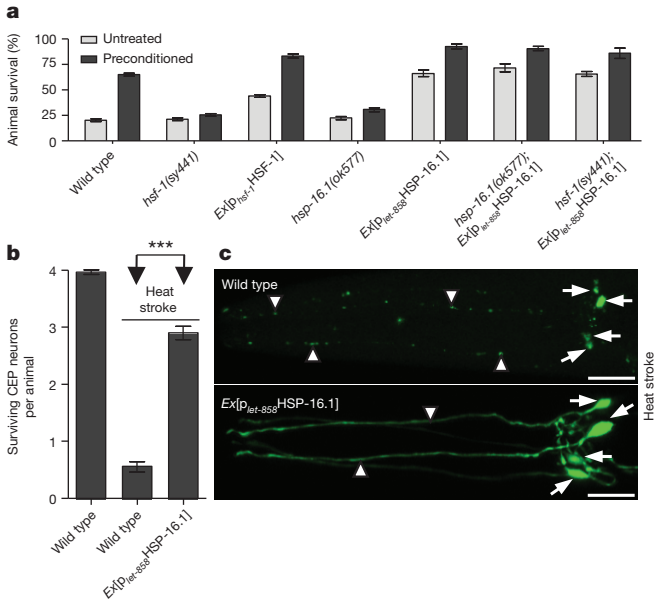


**Figure 1 | Heat preconditioning protects against extreme thermal stress through HSF-1 and HSP-16.1.** **a**, Survival of wild-type animals, *hsf-1(sy441)* or *hsp-16.1(ok577)* mutants, animals overexpressing *hsf-1* (*Ex*[$p_{hsf\text{-}1}$HSF-1]) or *hsp-16.1* (*Ex*[$p_{let\text{-}858}$HSP-16.1]), and *hsf-1* and *hsp-16.1* mutants overexpressing *hsp-16.1* after heat stroke, either without (untreated) or after preconditioning ($n = 350$ animals per assay; $P < 0.001$ for wild-type untreated versus preconditioned, $P > 0.05$ for *hsf-1(sy441)* or *hsp-16.1(ok577)* untreated versus preconditioned, $P < 0.001$ for wild-type untreated versus *Ex*[$p_{hsf\text{-}1}$HSF-1] or *Ex*[$p_{let\text{-}858}$HSP-16.1] untreated, $P < 0.001$ for *hsp-16.1(ok577)* untreated versus *hsp-16.1(ok577);Ex*[$p_{let\text{-}858}$HSP-16.1] untreated, $P < 0.001$ for *hsf-1(sy441)* untreated versus *hsf-1(sy441);Ex*[$p_{let\text{-}858}$HSP-16.1] untreated; two-way analysis of variance (ANOVA)). **b**, Survival of anterior CEP (cephalic) dopaminergic neurons of wild-type animals, and animals overexpressing *hsp-16.1* under heat stroke conditions ($n = 350$ animals per assay; $P < 0.001$ for wild-type heat-stroked versus *Ex*[$p_{let\text{-}858}$HSP-16.1] heat-stroked animals; unpaired *t*-test; ***$P < 0.001$). Error bars, mean ± s.e.m. **c**, Images of the head region of wild-type animals (top panel) and animals overexpressing *hsp-16.1* (bottom panel) after heat stroke. Remnants of neuron cell bodies (arrows) and axonal beading (arrowheads) are seen in wild-type animals (top panel). Both soma (arrows) and axonal (arrowheads) architecture is preserved in animals overexpressing *hsp-16.1*. Scale bar, 20 μm.

Fig. 6a). HSF-1, which mediates intrinsic thermotolerance[12], is also required for the resistance of ILS mutants to heat stroke (Supplementary Fig. 6a). In addition to HSF-1, thermotolerance conferred by low ILS is mediated by the FOXO (forkhead box protein O) transcription factor DAF-16, which translocates to the nucleus under stress[13]. We found that DAF-16 accumulates in the nucleus after preconditioning (Supplementary Fig. 6b, c). Such relocalization of DAF-16 is consistent with a synergistic effect of HSF-1 and DAF-16 on heat-shock protein (HSP) gene promoters that facilitates their maximal expression[14]. Indeed, DAF-16 is partly required for protection against heat stroke by preconditioning or low ILS (Supplementary Fig. 6a).

We also tested the requirement for other key stress response regulators; SKN-1, which mediates oxidative stress resistance, and the hypoxia inducible factor HIF-1. After activation, SKN-1 translocates to the nucleus[15]. We did not detect nuclear accumulation of SKN-1 after preconditioning (Supplementary Fig. 6d). Moreover, SKN-1 is dispensable for cytoprotection by preconditioning or low ILS (Supplementary Fig. 6a, e). HIF-1 is also not needed for the protective effect of preconditioning (Supplementary Fig. 6f). Based on these findings, we conclude that HSF-1 specifically promotes survival under extreme thermal stress, following preconditioning at intermediate temperature.

After activation, HSF-1 induces expression of genes encoding HSPs, which protect cells from various cytotoxic conditions[16,17]. Based on their molecular mass, HSPs are classified into six main families[18]. A plausible mechanism pertinent to the strong shielding effect of preconditioning, involves the coordinated upregulation of batteries of heat-shock genes by HSF-1. To test this notion, we surveyed key representatives of all main *C. elegans* heat-shock-protein families for their role in heat-stress resistance acquired after preconditioning. Instead of a distributed contribution from several HSPs, we found that HSP-16.1, HSP-16.41 and DNJ-19 are primarily needed for acquired tolerance to heat stroke (Fig. 1a and Supplementary Fig. 7a). However, among the corresponding genes, only *hsp-16.1* and *hsp-16.41* show significant upregulation after preconditioning ($P < 0.001$ untreated versus preconditioned, unpaired *t*-test), whereas *dnj-19* is constitutively expressed, even under control conditions (Supplementary Fig. 7b). DNJ-19 is a co-chaperone that modulates the activity of HSP-70. We found that *hsp-70* expression is similarly elevated, and not subject to regulation by preconditioning (Supplementary Fig. 7b). Of the two *hsp* genes that are specifically induced by preconditioning, only overexpression of *hsp-16.1* conferred significant protection, bypassing the requirement for preconditioning to suppress necrosis and increase animal survival after heat stroke. Moreover, it further potentiated thermotolerance after preconditioning (Fig. 1 and Supplementary Figs 2 and 7c).

HSP-16.1 belongs to the family of α-crystallin domain-containing small heat shock proteins (sHSPs) that are strongly induced under heat stress or low insulin signalling, and contribute to stress resistance and longevity in *C. elegans*[14,19,20]. Transcriptional upregulation of *hsp-16.1* after preconditioning is fully dependent on HSF-1 (Supplementary Fig. 8a). In contrast, induction of *hsp-16.1* expression by low ILS is not abolished by loss of DAF-16 (Supplementary Fig. 8b).

Overexpression of *hsp-16.1* under the control of a heterologous, non-heat-shock-responsive promoter, bypasses the requirement for HSF-1 to defend against heat stroke (Fig. 1a). Our findings show that HSP-16.1 is specifically induced during preconditioning, and is both necessary and sufficient for resistance to hyperthermia. Other HSPs that seem also to be needed for extreme heat tolerance are either not specifically induced (for example, HSP-70 and DNJ-19) or are not sufficient for protection (HSP-16.41).

## PMR-1 is required for hormetic protection

Typically, sHSPs are ubiquitously expressed and show widespread subcellular distribution[21]. Intriguingly, HSP-16.1 shows distinct localization to the medial Golgi of several cell types and is absent from other subcellular sites, including the closely related *trans*-Golgi and endosomes (Fig. 2a and Supplementary Figs 9a–d and 10a). HSP-16.41 displays a similar subcellular localization pattern (Supplementary Fig. 10b). This highly compartmentalized distribution is maintained under stress conditions in different genetic backgrounds (Supplementary Fig. 10c, d), suggesting that the two sHSPs function specifically in the medial Golgi to battle heat stress.

The Golgi apparatus is the main organelle for protein sorting and post-translational modification of proteins and lipids[22]. In addition, together with the endoplasmic reticulum and mitochondria, the Golgi is a major cellular $Ca^{2+}$ reservoir, facilitating cellular ion homeostasis[23–25]. Perturbation of intracellular calcium concentration ($[Ca^{2+}]_i$) homeostasis has been implicated in necrotic cell death, both in mammals and *C. elegans*[26,27]. We considered whether heat stroke might inflict necrosis by diminishing the capacity of cells to maintain low $[Ca^{2+}]_i$ levels under noxious thermal stress. To test this hypothesis, we knocked down the *itr-1* gene encoding the inositol-1,4,5-trisphosphate receptor ($InsP_3R$) channel, which mediates $Ca^{2+}$ trafficking out of both the Golgi and the endoplasmic reticulum[28]. $InsP_3R$ deficiency increased both intrinsic and acquired resistance to heat stroke (Fig. 2b). We found a similar effect after treatment of animals with dantrolene, a compound that inhibits $Ca^{2+}$ release from

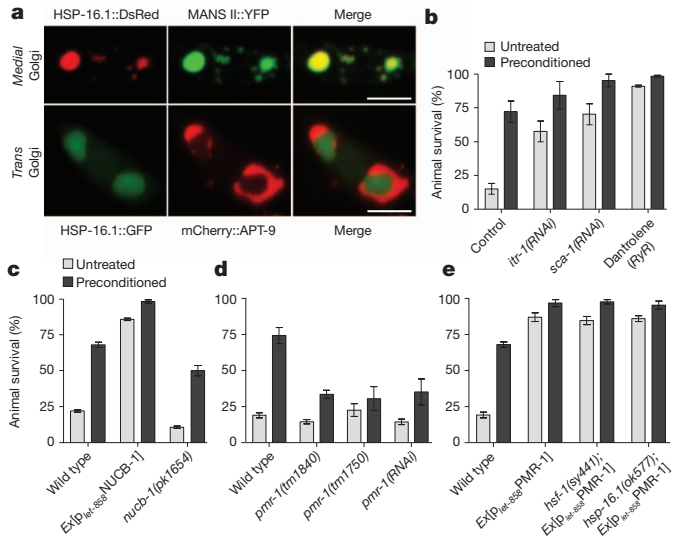


**Figure 2 | HSP-16. 1 localizes to the medial Golgi and functions together with PMR-1 to mediate the protective effect of preconditioning against heat stroke.** **a**, Images (cell bodies) of *C. elegans* neurons expressing fluorescently tagged HSP-16.1 along with medial (top row, middle panel) or *trans*-Golgi (bottom row, middle panel) markers. Scale bar, 6 μm. **b**, Survival of animals deficient for ITR-1 or SCA-1 (*itr-1(RNAi)*, *sca-1(RNAi)*), or animals exposed to dantrolene after heat stroke, either without (untreated) or after preconditioning ($n = 300$ animals per group; $P < 0.001$ for wild-type untreated (control) versus *itr-1(RNAi)*, *sca-1(RNAi)* or dantrolene-exposed; two-way ANOVA). **c**, Survival of wild-type animals, *nucb-1(pk1654)* mutants or animals overexpressing *nucb-1* (*Ex*[$p_{let\text{-}858}$NUCB-1]) after heat stroke, either without (untreated) or after preconditioning ($n = 300$ animals per assay; $P < 0.001$ for wild-type untreated versus *Ex*[$p_{let\text{-}858}$NUCB-1] untreated, $P < 0.01$ for wild-type untreated versus *nucb-1(pk1654)* untreated; two-way ANOVA). **d**, Survival of animals depleted for PMR-1 (*pmr-1(tm1840)* and *pmr-1(tm1750)* mutants, or *pmr-1(RNAi)* animals) under heat stroke, either without (untreated) or after preconditioning ($n = 800$ animals per assay; $P < 0.001$ for wild-type preconditioned versus *pmr-1(tm1840)*, *pmr-1(tm1750)* or *pmr-1(RNAi)* preconditioned; two-way ANOVA). **e**, Survival of wild-type animals and *hsf-1(sy441)* and *hsp-16.1(ok577)* mutants overexpressing *pmr-1* (*Ex*[$p_{let\text{-}858}$PMR-1]) under heat stroke, either without (untreated) or after heat preconditioning ($n = 300$ animals per assay; $P < 0.001$ for wild-type untreated versus *Ex*[$p_{let\text{-}858}$PMR-1], *hsf-1(sy441);Ex*[$p_{let\text{-}858}$PMR-1] or *hsp-16.1(ok577);Ex*[$p_{let\text{-}858}$PMR-1] untreated; two-way ANOVA). Error bars, mean ± s.e.m.

the Golgi and the endoplasmic reticulum, through the ryanodine receptor (RyR), or EGTA, a $Ca^{2+}$ chelator (Fig. 2b and Supplementary Fig. 11). Hence, moderating $[Ca^{2+}]_i$ levels by blocking release of Golgi and endoplasmic reticulum $Ca^{2+}$ stores, confers protection against thermal damage.

Ostensibly at odds with this idea, we observed a similar protective effect by knock down of *sca-1*, a gene encoding the sarco-endoplasmic reticulum $Ca^{2+}$ ATPase (SERCA), which pumps $Ca^{2+}$ from the cytoplasm into both the Golgi and the endoplasmic reticulum (Fig. 2b). Inhibition of SERCA induces endoplasmic reticulum stress and the unfolded protein response (UPR) pathway, leading to adaptation and survival[29,30]. We speculated that activation of the $UPR^{ER}$ (UPR in the endoplasmic reticulum) may account for the paradoxical cytoprotection. To test this hypothesis, we monitored the $UPR^{ER}$ after downregulation of SERCA, by means of an $UPR^{ER}$ indicator[31]. SCA-1 depletion resulted in strong induction of $UPR^{ER}$ (Supplementary Fig. 12a). We then tested whether elevated $UPR^{ER}$ is sufficient to confer protection against heat stroke. Indeed, *xbp-1* mutants, which display marked constitutive increase of $UPR^{ER}$ under physiological conditions[32], are resistant to heat stroke (Supplementary Fig. 12b). However, we found that preconditioning does not activate $UPR^{ER}$ (Supplementary Fig. 13a, b), suggesting that induction of $UPR^{ER}$ is not responsible for the protective effect of preconditioning. We also examined the involvement of mitochondrial UPR ($UPR^{mt}$), using a $p_{hsp\text{-}60}$GFP (green fluorescent protein) reporter[33]. Similar to the $UPR^{ER}$, the $UPR^{mt}$ is not activated by preconditioning (Supplementary Fig. 13c, d). Our findings indicate that preconditioning, as implemented in our assay, is highly specific in activating solely the heat-shock-response pathway, without engaging other stress responses typically induced by prolonged incubation at elevated temperatures[34] (Supplementary Fig. 14a–d).

None of the above manipulations that render animals resistant to hyperthermia is specific to the Golgi, where HSP-16.1 localizes. To manipulate $Ca^{2+}$ homeostasis specifically at the Golgi, we measured survival of transgenic animals overexpressing nucleobindin 1 (NUCB-1), a Golgi-resident $Ca^{2+}$-buffering protein[35], after heat stroke. We found that sequestration and retention of $Ca^{2+}$ in the Golgi by nucleobindin is sufficient to protect from heat stroke, even without preconditioning. In contrast, animals deficient for NUCB-1 are sensitized to heat stroke-induced damage (Fig. 2c).

To further isolate and assess the contribution of the Golgi in $Ca^{2+}$ homeostasis, we examined animals lacking PMR-1, a Golgi-specific $Ca^{2+}$- and $Mn^{2+}$-transporting P-type ATPase[36] that colocalizes with HSP-16.1 (Supplementary Fig. 15). PMR-1 deficiency suppresses preconditioning-acquired resistance to heat stroke (Fig. 2d). Importantly, overexpression of PMR-1 is sufficient to promote survival after heat stroke even without preconditioning, bypassing the requirement for both HSF-1 and HSP-16.1 (Fig. 2e). In addition, *pmr-1* expression is not altered by loss of HSF-1 or HSP-16.1 (Supplementary Fig. 16). Therefore, PMR-1 functions downstream of HSF-1 and HSP-16.1 to protect from hyperthermia. Together, our findings indicate that heat acclimatization through preconditioning may improve cytoprotection and animal survival by augmenting cellular $Ca^{2+}$ homeostasis through the Golgi.

## A universal cytoprotective mechanism

We considered the capacity of the mechanism involving specific heat-shock-response components and the Golgi PMR-1 ATPase to defend against additional necrotic insults unrelated to thermal stress. Dominant gain-of-function mutations in specific neuronal ion channels such as the degenerin MEC-4 and the acetylcholine receptor channel subunit DEG-3 evoke degenerative, necrotic cell death in *C. elegans* that is analogous to excitotoxicity in mammals[27,37]. Hypoxic conditions and overexpression of aggregation-prone proteins such as α-synuclein, also trigger necrosis in the nematode[38,39]. We exposed animals to brief heat preconditioning, before assaying cell death induced by toxic proteins or survival under hypoxia (Supplementary Fig. 1b). Remarkably, preconditioning suppressed neurodegeneration triggered by hyperactive ion channels or by overexpression of human α-synuclein (Fig. 3a, b and Supplementary Fig. 17a). Moreover, preconditioning increased animal resistance to hypoxic conditions (Fig. 3c). Preconditioning does not alter the expression, stability or function of cytotoxic proteins to ameliorate cell death (Supplementary Fig. 17b–d). In addition, suppression of neurodegeneration is not a mere consequence of a developmental delay in the onset of cell death (Supplementary Fig. 17e). Therefore, the heat-shock-response pathway intervenes downstream of necrotic insults to block necrosis. Cytoprotection is mediated by HSF-1 and HSP-16.1, which are both necessary and sufficient to ameliorate necrotic cell death (Fig. 3d, e). Thus, induction of the HSF-1–HSP-16 axis generally protects against necrosis inflicted by diverse stressors.

How might the heat-shock response neutralize necrotic stimuli? Excitotoxic insults initiate neuronal necrosis through elevation of $[Ca^{2+}]_i$ and subsequent aberrant activation of specific $Ca^{2+}$-dependent calpain proteases. In turn, calpains promote cell destruction by facilitating lysosome rupture[6,27,40]. We found that overexpression of NUCB-1 suppresses excitotoxic cell death, indicating that $Ca^{2+}$ release from the Golgi contributes to neurodegeneration (Fig. 3f).

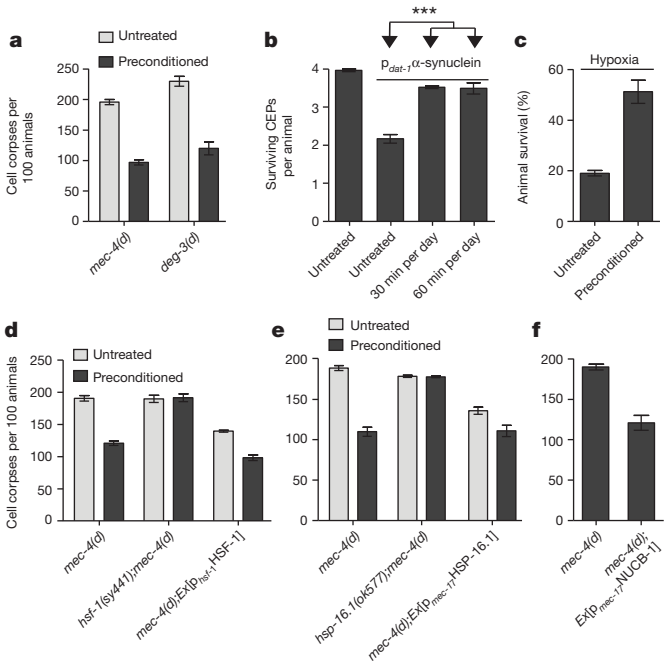


**Figure 3 | HSF-1 and HSP-16.1 mediate protection against necrosis inflicted by diverse insults upon preconditioning.** **a**, Number of neuron corpses at the L1 larval stage of development, per 100 animals carrying the neurotoxic dominant (*d*) *mec-4(d)* or *deg-3(d)* alleles, hatched from untreated or preconditioned eggs ($n = 350$ animals per assay; $P < 0.001$ for untreated versus preconditioned; two-way ANOVA). **b**, Dopaminergic neuron survival on the fifth day of adulthood in wild-type animals overexpressing α-synuclein, without or after receiving daily preconditioning (30 or 60 min per day; $n = 350$ animals per assay; $P < 0.001$ for untreated versus preconditioned; unpaired *t*-test; $^{***}P < 0.001$). **c**, Survival of wild-type animals after near-lethal treatment with sodium azide ($NaN_3$), either without or after preconditioning ($n = 350$ animals per assay; $P < 0.001$ for untreated versus preconditioned; unpaired *t*-test). **d**, Number of neuron corpses, at the L1 larval stage, per 100 *hsf-1(sy441);mec-4(d)* double mutants, and *mec-4(d)* animals overexpressing *hsf-1* hatched from untreated or preconditioned eggs ($n = 350$ animals per assay; $P > 0.05$ for *hsf-1(sy441);mec-4(d)* untreated versus preconditioned, $P < 0.001$ for *mec-4(d)* untreated versus *mec-4(d);Ex*[$p_{hsf-1}$HSF-1]; two-way ANOVA). **e**, Number of neuron corpses at the L1 larval stage, per 100 *hsp-16.1(ok577);mec-4(d)* double mutants, and *mec-4(d)* animals overexpressing *hsp-16.1* hatched from untreated or preconditioned eggs ($n = 350$ animals per assay; $P > 0.05$ for *hsp-16.1(ok577);mec-4(d)* untreated versus preconditioned, $P < 0.001$ for *mec-4(d)* untreated versus *mec-4(d);Ex*[$p_{mec-17}$HSP-16.1]; two-way ANOVA). **f**, Number of neuron corpses, at the L1 stage, per 100 *mec-4(d)* mutants overexpressing *nucb-1* ($n = 250$ animals; $P < 0.001$, unpaired *t*-test). Error bars, mean ± s.e.m.

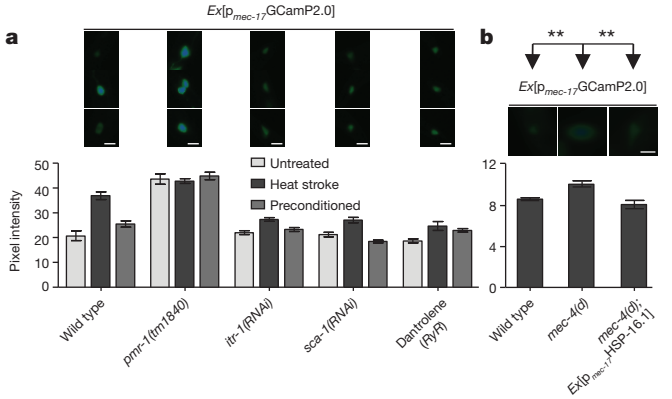


**Figure 4 | Preconditioning requires PMR-1 to alleviate heat-stroke-induced cytoplasmic $Ca^{2+}$ overload.** **a**, Fluorescence intensity of neurons expressing the $Ca^{2+}$ reporter GCaMP2.0, in wild-type animals, *pmr-1(tm1840)* mutants, and animals deficient for ITR-1, SCA-1 or treated with dantrolene, under normal conditions (untreated) and after heat stroke, either without or after preconditioning ($n = 60$ animals per assay; $P < 0.001$ for wild-type heat-stroked versus wild-type untreated or wild-type preconditioned; $P > 0.05$ for similar comparisons in mutant strains or after treatment with dantrolene; $P < 0.001$ for comparisons between *pmr-1(tm1840)* and other mutants or dantrolene treatment; two-way ANOVA). **b**, Fluorescence intensity of neurons, expressing GCaMP2.0, in wild-type animals, *mec-4(d)* mutants and *mec-4(d)* animals overexpressing *hsp-16.1* ($n = 150$ animals per assay; $P < 0.001$ for *mec-4(d)* versus wild-type or *mec-4(d);Ex*[$p_{mec-17}$HSP-16.1]; unpaired *t*-test $^{**}P < 0.01$). Representative images of neuron cell bodies are shown above each strain, for each condition. Scale bars, 10 μm. Error bars, mean ± s.e.m.

To examine whether heat stroke also triggers neurodegeneration by increasing $[Ca^{2+}]_i$, we monitored cytoplasmic $Ca^{2+}$ levels in *C. elegans* neurons after heat stroke. Similar to the cytotoxic dominant MEC-4 ion channel, extreme thermal stress causes a sharp increase in $[Ca^{2+}]_i$ levels (Fig. 4a, b). Heat preconditioning or inhibition of the $InsP_3R$ channel, the SERCA pump and the RyR channel quenches $[Ca^{2+}]_i$ elevation after subsequent heat stroke (Fig. 4a). Preconditioning by itself does not increase $Ca^{2+}$ levels (Supplementary Fig. 18). These findings parallel the protective effect of the above interventions against heat stroke-induced damage and death (Fig. 2b). In contrast, loss of the Golgi-specific PMR-1 $Ca^{2+}$ importer results in constitutive increase of $[Ca^{2+}]_i$ levels (Fig. 4a), consistent with the requirement for PMR-1 in preconditioning-acquired thermotolerance (Fig. 2d). Moreover, loss of PMR-1 exacerbates degenerin-induced necrotic cell death (Supplementary Fig. 17f). Thus, $Ca^{2+}$ import into the Golgi through PMR-1 is critical for survival after both heat stroke and excitotoxic insults. Combined, our data reveal a previously unsuspected and prominent role of the medial Golgi in maintaining $Ca^{2+}$ homeostasis under cytotoxic stress.

## A conserved pathway against hyperthermia

Our findings using a *C. elegans* hyperthermia model implicate specific heat-shock-response components and Golgi-mediated $Ca^{2+}$ homeostasis in resistance to a broad spectrum of necrotic insults, acquired after heat preconditioning. Has this protective mechanism been maintained during metazoan evolution or is it peculiar to the nematode? To address this question, we investigated whether key aspects of heat stroke neuropathology and heat preconditioning are conserved in mammalian neurons. To this end, we differentiated mouse embryonic stem cells into a homogeneous population of glutamatergic excitatory neurons[41]. Heat stroke induced pervasive death of embryonic-stem-cell-derived neurons (Fig. 5a, b and Supplementary Fig. 19a), and this effect could be largely prevented by heat preconditioning (Fig. 5a, b). We obtained similar results using primary cultures of mouse cortical (Fig. 5a, b) and striatal neurons (data not shown). In all cases, heat-stroked neurons showed axonal degeneration and other characteristics typical of necrotic death (Supplementary Fig. 19a, b).

Notably similar to the response in *C. elegans*, we found that overexpression of crystallin αA (CRYAA)[42], which co-localizes with the Golgi marker α-mannosidase II and the PMR1 ATPase (Supplementary Fig. 20a, b), was sufficient to protect mammalian neurons from heat-stroke-induced death, even in the absence of preconditioning (Fig. 5c). Finally, we tested whether the protective effect of preconditioning in mammalian neurons is also mediated by the PMR1 ATPase[43]. Heat stroke caused massive necrotic death and axonal degeneration in neurons expressing short hairpin RNAs (shRNAs) against *Pmr1*, even after preconditioning (Fig. 5d; Supplementary Fig. 21). Thus, knockdown of *Pmr1* abolishes the protective effect of preconditioning in mammalian neurons. These findings suggest that hormetic stress exposure engages a potent, evolutionarily conserved mechanism to defend against necrotic neurodegeneration, in metazoans as diverse as nematodes and mammals.

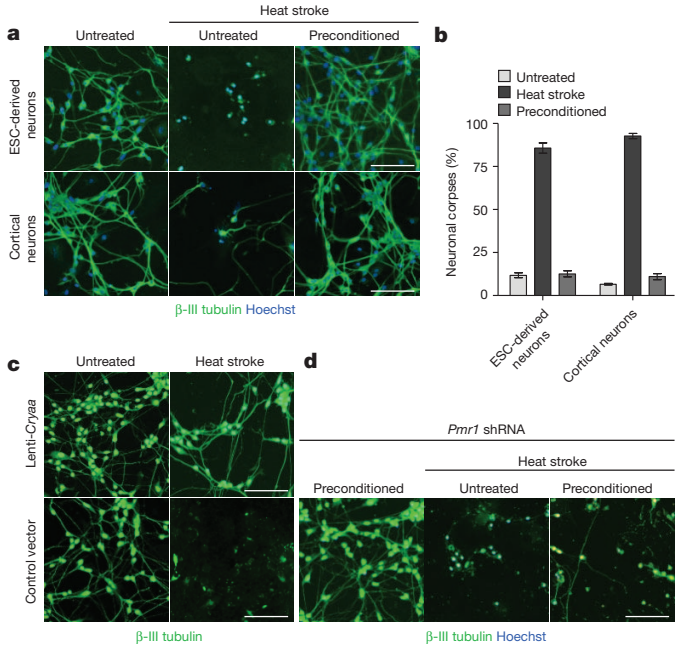


**Figure 5 | Heat preconditioning protects mammalian neurons against extreme thermal stress through crystallin αA and PMR1.** **a**, Images of embryonic stem cell (ESC)-derived neurons (top panels) and primary cortical neurons (bottom panels) immunostained for β-III tubulin, under normal conditions (untreated) and after heat stroke, either without or after preconditioning. Neuronal nuclei are stained with Hoechst. Scale bar, 100 μm. **b**, Corpses of ESC-derived and primary cortical neurons, under normal conditions (untreated) and after heat stroke, either without or after preconditioning ($n = 900$ neurons per assay, $P < 0.001$ for ESC-derived or cortical heat-stroked neurons versus corresponding preconditioned neurons; two-way ANOVA; error bars, mean ± s.e.m.). **c**, Images of ESC-derived neurons overexpressing *Cryaa*, or control vector after lentiviral infection, under normal conditions (untreated) and after heat stroke. Scale bar, 100 μm. **d**, Images of ESC-derived neurons after *Pmr1* downregulation, under normal conditions (untreated) and after heat stroke, either without or after preconditioning. Scale bar, 100 μm.

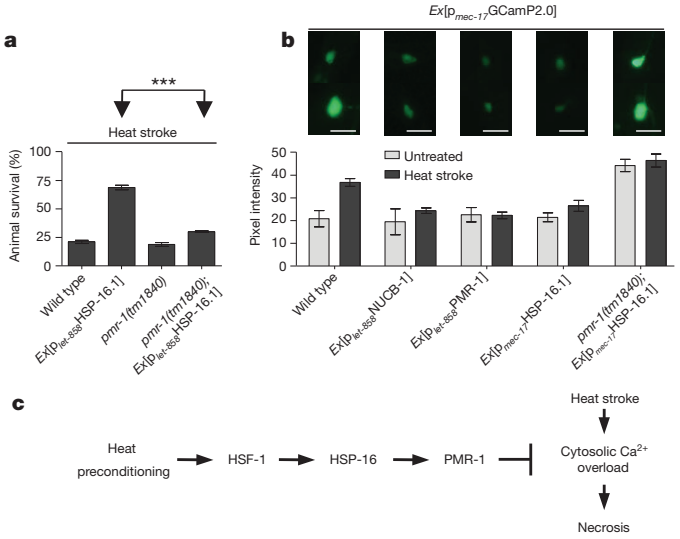


**Figure 6 | HSP-16.1 requires PMR-1 to suppress heat-stroke-induced necrosis and cytoplasmic $Ca^{2+}$ overload.** **a**, Survival of wild-type animals or *pmr-1(tm1840)* mutants overexpressing *hsp-16.1*, under heat stroke ($n = 400$ animals per assay; $P < 0.001$ for *Ex*[$p_{let\text{-}858}$HSP-16.1] versus *pmr-1(tm1840);Ex*[$p_{let\text{-}858}$HSP-16.1]; unpaired *t*-test; ***$P < 0.001$). **b**, Fluorescence intensity of touch receptor neurons expressing GCaMP2.0, in wild-type animals overexpressing *nucb-1*, *pmr-1* and *hsp-16.1*, or in *pmr-1(tm1840)* mutants overexpressing *hsp-16.1* under normal conditions (untreated), and after heat stroke ($n = 250$ animals per assay; $P < 0.001$ for wild-type untreated versus wild-type heat-stroked; $P > 0.05$ for *Ex*[$p_{let\text{-}858}$NUCB-1], *Ex*[$p_{let\text{-}858}$PMR-1], *Ex*[$p_{mec\text{-}17}$HSP-16.1] and *pmr-1(tm1840);Ex*[$p_{mec\text{-}17}$HSP-16.1] untreated versus heat-stroked; two-way ANOVA). Error bars, mean ± s.e.m. Representative images of neuron cell bodies are depicted above each strain, for each condition. Scale bar, 10 μm. **c**, Schematic representation of the protective pathway by which preconditioning augments resistance to heat-stroke-induced necrotic cell death. Arrows denote activation or upregulation. Blunt-ended arrow denotes inhibition.

## Discussion

In this report, we describe a versatile, genetically tractable *C. elegans* model of heat stroke and show that a single sHSP, HSP-16.1, is an effective general protector against multiple necrotic insults. HSP-16.1 localizes in the Golgi, where it functions together with the PMR-1 pump to prevent cytoplasmic $Ca^{2+}$ overload under extreme stress. Hormetic induction of HSP-16.1 expression by brief heat preconditioning is sufficient to fortify cells against diverse insults. Our findings, in both *C. elegans* and mammalian neurons indicate that an evolutionarily conserved pathway underlies the protective response (Fig. 6c). Three specific predictions derive from this model. First, that PMR-1 is required for resistance to extreme temperature, conferred by HSP-16.1 overexpression. Second, that HSP-16.1, NUCB-1 and PMR-1, which are exclusively localized in the Golgi, may promote survival by augmenting $Ca^{2+}$ sequestration into the Golgi and consequently maintaining subthreshold $[Ca^{2+}]_i$ levels. Third, importantly the model also predicts that moderation of $[Ca^{2+}]_i$ levels by HSP-16.1 requires PMR-1. We tested each of these predictions and found that, in complete agreement with the model, PMR-1 depletion diminishes the protective effect of HSP-16.1 overexpression (Fig. 6a). In addition, HSP-16.1, NUCB-1 or PMR-1 overexpression moderates $[Ca^{2+}]_i$ elevation induced by heat stroke (Fig. 6b). Moreover, the effect of HSP-16.1 is fully dependent on PMR-1 (Fig. 6b).

What is the molecular basis of HSP-16.1 protective function in the Golgi? sHSPs assemble into oligomeric complexes of variable stoichiometry and serve as molecular chaperones, efficiently binding denatured proteins and/or preventing irreversible protein aggregation and insolubilization[44]. Importantly, mammalian PMR1 is selectively impaired during ischaemic or reperfusion brain injury[45–47]. We propose that HSP-16.1 contributes to stabilize and protect the stress-labile PMR-1 pump, allowing for efficient clearance of $Ca^{2+}$ from the cytoplasm, after necrotic insults (Supplementary Fig. 22a–d).

Our study reveals a novel protective mechanism operating specifically in the Golgi to defend against a wide range of necrosis initiators. Given the strong evolutionary conservation of the proteins involved, this mechanism is probably relevant to related human pathologies. Indeed, noxious heat disrupts cytoplasmic calcium $Ca^{2+}$ absorption by subcellular organelles[48]. In addition, malignant hyperthermia susceptibility has been linked to mutations that cause resting $Ca^{2+}$ leakage to the cytoplasm through RyR[49,50]. Therefore, our findings could facilitate identification of candidate common intervention targets, in the effort to battle necrosis-related disorders in humans.

## METHODS SUMMARY

**Nematode heat stroke and preconditioning assays.** For heat stroke assays, synchronized populations of animals were grown under optimal growth conditions at 20 °C to young adult stage (early egg-laying). Synchronized populations were generated by transferring 20 to 30 gravid adult animals on fresh plates, letting them lay eggs for 1.5 h and then removing the adults. Animals were collected with M9 in 1.5-ml eppendorf tubes and incubated in 200 μl M9 buffer, at 39 °C for 15 min, in a water bath. Untreated worms were kept at 20 °C for the same time period. Survival rates were examined approximately 16 to 18 h post heat treatment. Animals that either moved freely or responded to tapping of the plate by moving the head or tail region of the body were considered survivors. To test whether prior activation of the heat-shock response (preconditioning) leads to increased survival against heat stroke, synchronized animals (prepared as described above) were incubated at 34 °C for 30 min, after a 20-min recovery incubation at 20 °C and then incubation at 39 °C for 15 min. Control animals

were kept at 20 °C after the recovery incubation. Survival rates were examined approximately 16-18 h post heat treatment at 39 °C. Survivors were scored as above.

**Full Methods** and any associated references are available in the online version of the paper.

**Received 30 March; accepted 16 July 2012.**
**Published online 12 September 2012.**

1. Patz, J. A., Campbell-Lendrum, D., Holloway, T. & Foley, J. A. Impact of regional climate change on human health. *Nature* **438,** 310–317 (2005).
2. Rowlands, D. J. *et al.* Broad range of 2050 warming from an observationally constrained large climate model ensemble. *Nature Geosci.* **5,** 256–260 (2012).
3. Bouchama, A. & Knochel, J. P. Heat stroke. *N. Engl. J. Med.* **346,** 1978–1988 (2002).
4. Dhopesh, V. P. & Burns, R. A. Loss of nerve conduction in heat stroke. *N. Engl. J. Med.* **294,** 557–558 (1976).
5. Hall, D. M. *et al.* Mechanisms of circulatory and intestinal barrier dysfunction during whole body hyperthermia. *Am. J. Physiol. Heart Circ. Physiol.* **280,** H509–H521 (2001).
6. Syntichaki, P., Xu, K., Driscoll, M. & Tavernarakis, N. Specific aspartyl and calpain proteases are required for neurodegeneration in *C. elegans*. *Nature* **419,** 939–944 (2002).
7. Xu, K., Tavernarakis, N. & Driscoll, M. Necrotic cell death in *C. elegans* requires the function of calreticulin and regulators of $Ca^{2+}$ release from the endoplasmic reticulum. *Neuron* **31,** 957–971 (2001).
8. Kourtis, N. & Tavernarakis, N. Cellular stress response pathways and ageing: intricate molecular relationships. *EMBO J.* **30,** 2520–2531 (2011).
9. Calabrese, E. J. Hormesis: a revolution in toxicology, risk assessment and medicine. *EMBO Rep.* **5,** S37–S40 (2004).
10. Åkerfelt, M., Morimoto, R. I. & Sistonen, L. Heat shock factors: integrators of cell stress, development and lifespan. *Nature Rev. Mol. Cell Biol.* **11,** 545–555 (2010).
11. McColl, G. *et al.* Insulin-like signaling determines survival during stress via posttranscriptional mechanisms in *C. elegans*. *Cell Metab.* **12,** 260–272 (2010).
12. Chiang, W. C., Ching, T. T., Lee, H. C., Mousigian, C. & Hsu, A. L. HSF-1 regulators DDL-1/2 link insulin-like signaling to heat-shock responses and modulation of longevity. *Cell* **148,** 322–334 (2012).
13. Lin, K., Hsin, H., Libina, N. & Kenyon, C. Regulation of the *Caenorhabditis elegans* longevity protein DAF-16 by insulin/IGF-1 and germline signaling. *Nature Genet.* **28,** 139–145 (2001).
14. Hsu, A. L., Murphy, C. T. & Kenyon, C. Regulation of aging and age-related disease by DAF-16 and heat-shock factor. *Science* **300,** 1142–1145 (2003).
15. An, J. H. & Blackwell, T. K. SKN-1 links *C. elegans* mesendodermal specification to a conserved oxidative stress response. *Genes Dev.* **17,** 1882–1893 (2003).
16. Lindquist, S. & Craig, E. A. The heat-shock proteins. *Annu. Rev. Genet.* **22,** 631–677 (1988).
17. Morimoto, R. I. Proteotoxic stress and inducible chaperone networks in neurodegenerative disease and aging. *Genes Dev.* **22,** 1427–1438 (2008).
18. Morimoto, R. I. Regulation of the heat shock transcriptional response: cross talk between a family of heat shock factors, molecular chaperones, and negative regulators. *Genes Dev.* **12,** 3788–3796 (1998).
19. Walker, G. A. & Lithgow, G. J. Lifespan extension in *C. elegans* by a molecular chaperone dependent upon insulin-like signals. *Aging Cell* **2,** 131–139 (2003).
20. Morley, J. F. & Morimoto, R. I. Regulation of longevity in *Caenorhabditis elegans* by heat shock factor and molecular chaperones. *Mol. Biol. Cell* **15,** 657–664 (2004).
21. Haslbeck, M., Franzmann, T., Weinfurtner, D. & Buchner, J. Some like it hot: the structure and function of small heat-shock proteins. *Nature Struct. Mol. Biol.* **12,** 842–846 (2005).
22. Lowe, M. Structural organization of the Golgi apparatus. *Curr. Opin. Cell Biol.* **23,** 85–93 (2011).
23. Missiaen, L., Dode, L., Vanoevelen, J., Raeymaekers, L. & Wuytack, F. Calcium in the Golgi apparatus. *Cell Calcium* **41,** 405–416 (2007).
24. Van Baelen, K. *et al.* The $Ca^{2+}/Mn^{2+}$ pumps in the Golgi apparatus. *Biochim. Biophys. Acta* **1742,** 103–112 (2004).
25. Pinton, P., Pozzan, T. & Rizzuto, R. The Golgi apparatus is an inositol 1,4,5-trisphosphate-sensitive $Ca^{2+}$ store, with functional properties distinct from those of the endoplasmic reticulum. *EMBO J.* **17,** 5298–5308 (1998).
26. McCall, K. Genetic control of necrosis — another type of programmed cell death. *Curr. Opin. Cell Biol.* **22,** 882–888 (2010).
27. Syntichaki, P. & Tavernarakis, N. The biochemistry of neuronal necrosis: rogue biology? *Nature Rev. Neurosci.* **4,** 672–684 (2003).
28. Michelangeli, F., Ogunbayo, O. A. & Wootton, L. L. A plethora of interacting organellar $Ca^{2+}$ stores. *Curr. Opin. Cell Biol.* **17,** 135–140 (2005).
29. Ferri, K. F. & Kroemer, G. Organelle-specific initiation of cell death pathways. *Nature Cell Biol.* **3,** E255–E263 (2001).
30. Rutkowski, D. T. *et al.* Adaptation to ER stress is mediated by differential stabilities of pro-survival and pro-apoptotic mRNAs and proteins. *PLoS Biol.* **4,** e374 (2006).
31. Calfon, M. *et al.* IRE1 couples endoplasmic reticulum load to secretory capacity by processing the XBP-1 mRNA. *Nature* **415,** 92–96 (2002).
32. Richardson, C. E., Kinkel, S. & Kim, D. H. Physiological IRE-1-XBP-1 and PEK-1 signaling in *Caenorhabditis elegans* larval development and immunity. *PLoS Genet.* **7,** e1002391 (2011).
33. Yoneda, T. *et al.* Compartment-specific perturbation of protein handling activates genes encoding mitochondrial chaperones. *J. Cell Sci.* **117,** 4055–4066 (2004).
34. Lithgow, G. J., White, T. M., Melov, S. & Johnson, T. E. Thermotolerance and extended life-span conferred by single-gene mutations and induced by thermal stress. *Proc. Natl Acad. Sci. USA* **92,** 7540–7544 (1995).
35. Lin, P., Yao, Y., Hofmeister, R., Tsien, R. Y. & Farquhar, M. G. Overexpression of CALNUC (nucleobindin) increases agonist and thapsigargin releasable $Ca^{2+}$ storage in the Golgi. *J. Cell Biol.* **145,** 279–289 (1999).
36. Van Baelen, K., Vanoevelen, J., Missiaen, L., Raeymaekers, L. & Wuytack, F. The Golgi PMR1 P-type ATPase of *Caenorhabditis elegans*. Identification of the gene and demonstration of calcium and manganese transport. *J. Biol. Chem.* **276,** 10683–10691 (2001).
37. Yamashima, T. *et al.* Sustained calpain activation associated with lysosomal rupture executes necrosis of the postischemic CA1 neurons in primates. *Hippocampus* **13,** 791–800 (2003).
38. Cao, S., Gelwix, C. C., Caldwell, K. A. & Caldwell, G. A. Torsin-mediated protection from cellular stress in the dopaminergic neurons of *Caenorhabditis elegans*. *J. Neurosci.* **25,** 3801–3812 (2005).
39. Scott, B. A., Avidan, M. S. & Crowder, C. M. Regulation of hypoxic death in *C. elegans* by the insulin/IGF receptor homolog DAF-2. *Science* **296,** 2388–2391 (2002).
40. Yamashima, T. Implication of cysteine proteases calpain, cathepsin and caspase in ischemic neuronal death of primates. *Prog. Neurobiol.* **62,** 273–295 (2000).
41. Bibel, M., Richter, J., Lacroix, E. & Barde, Y. A. Generation of a defined and uniform population of CNS progenitors and neurons from mouse embryonic stem cells. *Nature Protocols* **2,** 1034–1043 (2007).
42. Brady, J. P. *et al.* Targeted disruption of the mouse αA-crystallin gene induces cataract and cytoplasmic inclusion bodies containing the small heat shock protein αB-crystallin. *Proc. Natl Acad. Sci. USA* **94,** 884–889 (1997).
43. Shull, G. E. *et al.* Physiological functions of plasma membrane and intracellular $Ca^{2+}$ pumps revealed by analysis of null mutants. *Ann. NY Acad. Sci.* **986,** 453–460 (2003).
44. van Montfort, R. L., Basha, E., Friedrich, K. L., Slingsby, C. & Vierling, E. Crystal structure and assembly of a eukaryotic small heat shock protein. *Nature Struct. Biol.* **8,** 1025–1030 (2001).
45. Gidday, J. M. Cerebral preconditioning and ischaemic tolerance. *Nature Rev. Neurosci.* **7,** 437–448 (2006).
46. Lehotský, J. *et al.* Ion transport systems as targets of free radicals during ischemia reperfusion injury. *Gen. Physiol. Biophys.* **21,** 31–37 (2002).
47. Pavlíková, M. *et al.* Alterations induced by ischemic preconditioning on secretory pathways $Ca^{2+}$-ATPase (SPCA) gene expression and oxidative damage after global cerebral ischemia/reperfusion in rats. *Cell. Mol. Neurobiol.* **29,** 909–916 (2009).
48. Greffrath, W., Kirschstein, T., Nawrath, H. & Treede, R. Changes in cytosolic calcium in response to noxious heat and their relationship to vanilloid receptors in rat dorsal root ganglion neurons. *Neuroscience* **104,** 539–550 (2001).
49. Lanner, J. T. e. t. a. l. AICAR prevents heat-induced sudden death in RyR1 mutant mice independent of AMPK activation. *Nature Med.* **18,** 244–251 (2012).
50. Protasi, F., Paolini, C. & Dainese, M. Calsequestrin-1: a new candidate gene for malignant hyperthermia and exertional/environmental heat stroke. *J. Physiol.* **587,** 3095–3100 (2009).

**Supplementary Information** is available in the online version of the paper.

**Acknowledgements** We thank K. Georgila, K. Palikaras and E. Bessa for help with cell-death assays, A. Pasparaki for technical support with experiments and C. Olendrowitz for help with electron microscopy. We thank S. Eimer for providing the Golgi and endosomal reporter constructs and for support with the electron microscopy, N. Chronis for providing the pN1-GCaMP2.0 plasmid, G. Caldwell for the α-synuclein-expressing *C. elegans* strain and K. Palikaras for the *skn-1* RNAi plasmid. We thank J. Vanoevelen and F. Wuytack for the antibody against PMR-1, S. Mitrovic for the antibody against mannosidase II, G. Sourvinos for lentiviral plasmids, and S. Gascon for the pLV plasmid. Some nematode strains used in this work were provided by the *Caenorhabditis* Genetics Center, which is funded by the National Center for Research Resources (NCRR) of the National Institutes of Health (NIH), and S. Mitani (National Bioresource Project) in Japan. We thank A. Fire for plasmid vectors. V.N. is supported by an European Molecular Biology Organization (EMBO) Long Term Fellowship. This work was funded by grants from the European Research Council (ERC) and the European Commission 7th Framework Programme.

**Author Contributions** N.K., V.N. and N.T. designed and carried out experiments. N.K. and N.T. analysed data and wrote the manuscript.

**Author Information** Reprints and permissions information is available at www.nature.com/reprints. The authors declare no competing financial interests. Readers are welcome to comment on the online version of the paper. Correspondence and requests for materials should be addressed to N.T. (tavernarakis@imbb.forth.gr).

## METHODS

**Strains and genetics.** We followed standard procedures for *C. elegans* strain maintenance[51]. The nematode rearing temperature was kept at 20 °C, unless noted otherwise. The following strains were used in this study: N2: wild-type Bristol isolate, MT1522: *ced-3(n717)IV*, KJ216: *crt-1(jh101)V*, *clp-1(tm690)III*, RB2035: *asp-4(ok2693)X*, TU1747: *deg-3(u662)V* (referred to in the text as *deg-3(d)*), *mec-4(u231)X* (referred to in the text as *mec-4(d)*), PS3551: *hsf-1(sy441)I*, RB791: *hsp-16.1(ok577)V*, VC475: *hsp-16.2(gk249)V*, VC1099: *hsp-4(gk514)II*, RB1104: *hsp-3(ok1083)X*, *hsp-6(tm515)V*, *hsp-16.41(tm1093)V*, *hsp-70(tm2318)I*, VC914: *daf-21(ok1333)V*, VC1348: *dnj-19(gk649)V*, NL4266: *nucb-1(pk1654)X*, CB1370: *daf-2(e1370)III*, DR26: *daf-16(m26)I*, *daf-16(m26)I;daf-2(e1370)III*, ZG31: *hif-1(ia4)V*, SJ17: *xbp-1(zc12)III*, SJ4005: N2;*Is*[$p_{hsp4}$GFP]*V*, SJ4058: N2;*Is*[$p_{hsp-60}$GFP]*V*, EU1: *skn1(zu67)IV/nT1(IV;V)*, EU31: *skn1(zu135)IV/nT1(IV;V)*, EU40: *skn1(zu129)IV/nT1(IV;V)*, *pmr-1(tm1840)I*, *pmr-1(tm1750)I*, CF1824: *muEx265* [pAL9($p_{hsf-1}$HSF-1) pPD97.93($p_{myo-3}$GFP)]. The following strains were examined for neurodegeneration in this study: *hsf-1(sy441)I;mec-4(u231)X*, *hsp-16.1(ok577)V;mec-4(u231)X*, *mec-4(u231)X;Ex*[$p_{hsf-1}$HSF-1], *mec-4(u231)X;Ex*[$p_{mec-17}$HSP-16.1], *mec-4(u231)X;Ex*[$p_{mec-17}$NUCB-1] *mec-4(u231)X;Is*[$p_{mec-4}$GFP], *pmr-1(tm1840)I;mec-4(u231)X*. To assay the expression of aspartyl proteases after heat stroke we examined the N2;*Ex*[$p_{asp-4}$ASP-4::GFP] transgenic animals. To verify that preconditioning does not interfere with the expression or localization and stability of the toxic MEC-4 channel, we examined the following transgenic strains: N2;*Is*[$p_{mec-4}$GFP] and N2;*Is*[$p_{mec-4}$MEC-4::GFP]. The following strains were examined in co-localization experiments: N2;*Ex*[$p_{mec-17}$HSP-16.1::DsRed;$p_{rab-3}$manosidase II::GFP], N2;*Ex*[$p_{mec-17}$HSP-16.1::GFP;$p_{rab-3}$mCherry::APT-9], N2;*Ex*[$p_{mec-17}$HSP-16.1::DsRed;$p_{rab-3}$2xfyve domain::GFP] and N2;*Ex*[$p_{mec-17}$PMR-1::DsRed;$p_{mec-17}$HSP-16.1::GFP]. To assay the localization of DAF-16 and SKN-1 after heat preconditioning, we examined CF1139: *daf16(mu86)I;Is*[$p_{daf16}$DAF-16a::GFP] and LD1: N2;*Is*[$p_{skn1}$SKN-1b/c::GFP] transgenic animals. To investigate the localization of HSP-16.41 in neurons, we examined N2;*Ex*[$p_{mec-17}$HSP-16.41::GFP] transgenic animals. To examine the localization of HSP1-6.1 in *hsf-1(sy441)I* and *daf-2(e1370)III* mutants and *muEx265* [pAL9($p_{hsf-1}$HSF-1) pPD97.93($p_{myo-3}$GFP)] transgenic animals, the following strains were used: *hsf-1(sy441)I;Ex*[$p_{mec-17}$HSP-16.1::GFP], *daf-2(e1370)III;Ex*[$p_{mec-17}$HSP-16.1::GFP] and *muEx265* [pAL9($p_{hsf-1}$HSF-1);$p_{mec-17}$HSP-16.1::GFP]. To monitor autophagy induction after heat preconditioning and heat stroke, we used the QU1: N2;*Ex*[$p_{lgg-1}$GFP::LGG-1] strain. The following strains were used for monitoring calcium levels in touch receptor neurons: N2;*Ex*[$p_{mec-17}$GCamP2.0], N2;*Ex*[$p_{mec-17}$GCamP2.0;$p_{mec-17}$HSP-16.1], N2;*Ex*[$p_{mec-17}$GCamP2.0;$p_{let-858}$NUCB-1], N2;*Ex*[$p_{mec-17}$GCamP2.0;$p_{let-858}$PMR-1], *pmr-1(tm1840)I;Ex*[$p_{mec-17}$GCamP2.0], *pmr-1(tm1840)I;Ex*[$p_{mec-17}$GCamP2.0;$p_{mec-17}$HSP-16.1] *mec-4(u231)X;Ex*[$p_{mec-17}$GCamP2.0], *mec-4(u231)X;Ex*[$p_{mec-17}$GCamP2.0;$p_{mec-17}$HSP-16.1]. To investigate the protective role of global expression of *HSP-16.1* against heat stroke, we examined N2;*Ex*[$p_{let-858}$HSP-16.1], *hsp 16.1(ok577);Ex*[$p_{let-858}$HSP-16.1], *hsf-1(sy441);Ex*[$p_{let-858}$HSP-16.1], *Is*[$p_{dat-1}$GFP];*Ex*[$p_{let-858}$HSP-16.1] and *pmr-1(tm1840)I;Ex*[$p_{let-858}$HSP-16.1] transgenic animals. To investigate the role of global expression of *nucb-1* against heat stroke, we examined N2;*Ex*[$p_{let-858}$NUCB-1] transgenic animals. To investigate the protective role of global expression of *pmr-1* against heat stroke, we examined N2;*Ex*[$p_{let-858}$PMR-1], *hsf-1(sy441);Ex*[$p_{let-858}$PMR-1] and *hsp-16.1(ok577);Ex*[$p_{let-858}$PMR-1]. To assay the protective effect of global expression of *hsp-16.41* and *dnj-19* against heat stroke, we examined N2;*Ex*[$p_{let-858}$HSP-16.41] and N2;*Ex*[$p_{let-858}$DNJ-19] transgenic animals. To survey the protective role of preconditioning in a *C. elegans* model of Parkinson's disease, we tested the UA44 *Is*[baln1; $p_{dat-1}$α-syn, $p_{dat-1}$GFP] transgenic animals expressing α-synuclein in nematode dopaminergic neurons[52].

**Molecular cloning.** For $p_{mec-17}$HSP-16.1, an *Xma*I-*Kpn*I fragment containing the *hsp-16.1* coding region plus 536 base pairs (bp) of the 3′ untranslated region (UTR) was amplified from *C. elegans* genomic DNA using the primers 5′-CCCGGGATGTCACTTTACCACTATTTCCG-3′ and 5′-GGTACCTATCC ATGTTCCAATTCCTGC-3′ and was cloned into the corresponding sites of $p_{mec-17}$GFP. Construction of $p_{mec-17}$GFP has been described previously[53]. The $p_{mec-17}$HSP-16.1 construct was injected into the gonads of *mec-4(u231)* animals together with a plasmid that carries a $p_{myo-2}$GFP reporter fusion, expressing GFP in the pharyngeal muscle cells, as a transformation marker. To generate the $p_{mec-17}$HSP-16.1::GFP reporter construct, we fused a *Sma*I-*Age*I fragment containing the coding sequence of *hsp-16.1*, amplified from *C. elegans* genomic DNA using the primers 5′-CCCGGGATGTCACTTTACCACTATTTCCG-3′ and 5′-ACCGGTCCTTCAGAAGTTTTTTGTTCAACG-3′, at the amino terminus of GFP of the $p_{mec-17}$GFP. The translational $p_{mec-17}$HSP-16.1::GFP fusion construct was co-injected with pRF4 (contains *rol-6(su1006)*) into the gonads of wild-type animals. To generate the $p_{let-858}$HSP-16.1 construct, a *Kpn*I-*Xma*I fragment containing the *hsp-16.1* coding region plus approximately 500 bp of 3′ UTR was amplified from *C. elegans* genomic DNA using the primers 5′-GGTACCATGTCACTTTACCACTATTTCCG-3′ and 5′-CCCGGGTATC CATGTTCCAATTCCTGC-3′and was inserted downstream of the *let-858* promoter of the L2865 plasmid vector. The $p_{let-858}$HSP-16.1 construct was injected into the gonads of wild-type animals together with a plasmid carrying the reporter gene $p_{unc-122}$GFP, which stains the coelomocytes of *C. elegans*. To generate the $p_{mec-17}$GCaMP2.0 construct the primers 5′-CTGCAGAGCAAAGACGGCAAG AACTG-3′ and 5′-CCCGGGGATCGAATCGTCTCACAAC-3′ were used to amplify a *Pst*I-*Xma*I fragment containing the promoter of *mec-17* (1643 bp) from *C. elegans* genomic DNA. In addition, the primers 5′-CCCGGGATGCGG GGTTCTCATCATC-3′ and 5′-GATATCTCACTTCGCTGTCATCATTTG-3′ were used to amplify an *Xma*I-*Eco*RV fragment containing the GCaMP2.0 coding region amplified from the pN1-GCaMP2.0 plasmid. The two amplified fragments were cloned into the pPD49.26 vector. The resulting plasmid construct was injected into the gonads of wild-type animals together with the reporter $p_{unc-122}$GFP. To generate the $p_{let-858}$HSP-16.1::GFP construct, the primers 5′-ACCGGTATGTCACTTTACCACTATTTCCG-3′ and 5′-ACCGGTCCTTC AGAAGTTTTTTGTTCAACG-3′ were used to amplify an *Age*I-flanked fragment containing the coding sequence of *hsp-16.1*, which was then inserted downstream of the *let-858* promoter in L3786 plasmid. The reporter construct was injected into the gonads of wild-type animals together with pRF4. To generate the $p_{mec-17}$NUCB-1 construct the primers 5′-GGATCCATGATTAAGCCTCT AGTC-3′ and 5′-CCATGGTAGATTGGTGAGGTAGTG-3′ were used to amplify a *Bam*HI-*Nco*I fragment containing the coding sequence of *nucb-1*, which was inserted downstream of the promoter of *mec-17* in the $p_{mec-17}$/pPD95.77 construct. The resulting construct was injected into the gonads of *mec-4(d)* animals together with the reporter $p_{unc-122}$GFP. To generate the $p_{let-858}$NUCB-1 construct, the primers 5′-TCTAGAATGATTAAGCCTCTAGTC-3′ and 5′-GGG CCCTAGATTGGTGAGGTAGTG-3′ were used to amplify an *Xba*I-*Apa*I fragment containing the coding sequence of *nucb-1*, which was inserted downstream of the *let-858* promoter of the L2865 plasmid vector. The $p_{let-858}$NUCB-1 construct was co-injected with pRF4 into the gonads of wild-type animals. To generate the $p_{let-858}$PMR-1 construct, the primers 5′-GCGGGGTACCATGA ATGGATCAGTGGCTCC-3′ and 5′-TTATGGGTATCCCGTATGG-3′ were used to amplify a *Kpn*I fragment containing the *pmr-1* complementary DNA, which was inserted downstream of the *let-858* promoter of the L2865 plasmid vector. The $p_{let-858}$PMR-1 construct was co-injected with pRF4 into the gonads of wild-type animals. To generate the $p_{mec-17}$PMR-1::DsRed reporter construct, the primers 5′-GCTCCCCCCGGGATGATTGAAACACTGACATC-3′ and 5′-CCCTAGACCGGTCCAATTCCGCTGACAGACAGGG-3′ were used to amplify an *Xma*I-*Age*I fragment containing the *pmr-1* cDNA, which was inserted at the N terminus of DsRed of the $p_{mec-17}$DsRed vector. The $p_{mec-17}$PMR-1::DsRed construct was co-injected with pRF4 into the gonads of wild-type animals. To generate the $p_{let-858}$HSP-16.41 construct, a *Xma*I-*Apa*I fragment containing the *hsp-16.41* coding region plus approximately 500 bp of the 3′ UTR was amplified from *C. elegans* genomic DNA using the primers 5′-CCCGGGATGCTCA TGCTCCGTTCTC-3′ and 5′-GGGCCCAGAAGTTTGGAGTCAGGAGG-3′ and was inserted downstream of the *let-858* promoter of the L2865 plasmid vector. The $p_{let-858}$HSP-16.41 construct was injected into the gonads of wild-type animals together with pRF4. To generate the $p_{let-858}$DNJ-19 construct, a *Xma*I-*Apa*I fragment containing the *dnj-19* coding region plus approximately 500 bp of the 3′ UTR was amplified from *C. elegans* genomic DNA using the primers 5′-CCCGGGATGTTTGGAGGTGGAAGTAG-3′ and 5′-GGGCCCCATGTGT GCAGTATAATGTG-3′ and was inserted downstream of the *let-858* promoter of the L2865 plasmid vector. The $p_{let-858}$DNJ-19 construct was injected into the gonads of wild-type animals together with pRF4. To generate the $p_{mec-17}$HSP-16.41::GFP reporter construct, we fused a *Xma*I-*Age*I fragment containing the coding sequence of *hsp-16.41*, amplified from *C. elegans* genomic DNA using the primers 5′-CCCGGGATGCTCATGCTCCGTTCTC-3′ and 5′ACCGGTCCATGTTTTGCAACAAAATTG-3′, at the N terminus of GFP of the $p_{mec-17}$GFP plasmid. The translational $p_{mec-17}$HSP-16.41::GFP fusion construct was co-injected with pRF4 into the gonads of wild-type animals. For engineering the *sca-1*, *itr-1* and *pmr-1* RNAi constructs, gene-specific fragments of interest were obtained by polymerase chain reaction (PCR) amplification directly from *C. elegans* genomic DNA using the sets of primers 5′-GCGG CCGCTAAGGAACTCGTGCCAGGAG-3′ and 5′-GTCGACACTTGGCGA CAGCAGTTCC-3′, 5′-GAATTCAGCCCAATGTCCGCAATCC-3′ and 5′-GA ATTCACACTCAGCGACCCGATACC-3′, 5′-AACTGCAGATTGAAACACT GACATC-3′ and 5′-CCGCTCGAGTACCTGAAACATTCCG-3′, respectively. The PCR-generated fragments were subcloned into the pL4440 plasmid vector and resulting constructs were transformed into HT115(DE3) *Escherichia coli* bacteria deficient for RNase E. Bacteria carrying an empty vector were used in control experiments. For *sca-1* and *itr-1* RNAi the effect can be severe, leading to

sterility of the animals. Lower incubation times during HT115 culture preparation might be required.

***C. elegans* cell-death assays.** To assay the protective role of preconditioning against necrosis triggered by hyperactive channels, *C. elegans* animals were grown under optimal growth conditions at 20 °C, to gravid adult stage. Animals were collected with M9 in 1.5-ml eppendorf tubes. After a brief centrifugation at 10,000*g*, M9 was removed and 0.5 ml of bleaching solution (7 ml $H_2O$, 1 ml NaOH 5 N and 2 ml bleach) was added. Animals were allowed to dissolve and the remaining eggs were collected by centrifugation for 25 s at 10,000*g* and washed twice with 1 ml M9. After washing, eggs were resuspended in 200 µl M9 and incubated for 25 min at 34 °C, in a water bath. Alternatively, eggs were subjected 3 times to 8-min preconditioning periods with 45 min periods of recovery twice between heat-shock sessions. Control animals were maintained at 20 °C for the duration of preconditioning. Control and preconditioned eggs were placed on nematode growth medium (NGM) plates and incubated at 20 °C until hatching. Animals were mounted in 2% agarose pads, anaesthetized with 10 mM sodium azide and observed using differential interference contrast (DIC) microscopy. To test whether preconditioning perturbs the function of MEC-4, wild-type animals were preconditioned as described previously, whereas the control population was maintained at 20 °C for the course of preconditioning. Preconditioned and control animals were assessed for responsiveness to gentle body touch, at the L4 stage. Animals received five sequential gentle touches with an eyelash in the anterior and posterior part of the body, and their responsiveness (indicated by the change in the direction of movement) was recorded. For time-course analysis of necrotic cell death, synchronized animal populations were obtained by collecting embryos from gravid adults after treatment with bleaching solution. These populations were divided in two. One subpopulation was preconditioned and the other was maintained at 20 °C for the duration of preconditioning. In each experiment, neuron corpses were counted in each subpopulation at a specific developmental stage. Developmental stages from L1 to L4 were examined. The total number of corpses was calculated as the sum of three counts for each subpopulation and developmental stage. To assess the effects of preconditioning in a *C. elegans* model of Parkinson's disease, NGM plates containing L4 staged animals were preconditioned daily for 30 or 60 min by immersing the plate in a water bath set at 34 °C. Dopaminergic neuron loss was monitored on the fifth day of adulthood by scoring for loss of fluorescence from neurons expressing GFP under the promoter of *dat-1*. Survival after heat stroke of dopaminergic neurons of *Is*[$p_{dat\text{-}1}$GFP];*Ex*[$p_{let\text{-}858}$HSP-16.1] young adult transgenic animals was assessed 5 h after the assay. Neurons showing soma or axonal degeneration were considered dead. For propidium iodide staining (a fluorescent dye excluded from viable cells and apoptotic corpses), young adult worms were incubated for 3 h in 10 µM propidium iodide (Sigma) in M9 buffer, after incubation at 39 °C for 15 min, and visualized using a compound epifluorescence microscope. For monitoring of induction of expression of the *asp-4* gene, young adult worms carrying the *asp-4*::GFP reporter fusion were incubated at 39 °C for 15 min and the expression of GFP in vacuolated cells was monitored after 3 h using a compound epifluorescence microscope.

***C. elegans* survival assays.** To investigate the protective role of preconditioning against hypoxic conditions, wild-type nematodes at the L4 stage of development were collected and washed 2 to 3 times with 1 ml M9, preconditioned for 15 min at 34 °C and left to recover for 10 min. Control animals were maintained at 20 °C for the duration of preconditioning. To induce hypoxia, control and preconditioned animals were incubated for 1 h at 25 °C, in 1 ml of 0.5 M freshly made $NaN_3$ (Sigma) in M9. Sodium azide is an inhibitor of the respiratory chain electron transport complex IV (cytochrome *c* oxidase) and simulates hypoxia. Worms were washed 3 times with 1 ml M9 and placed into NGM plates to recover. The percentage of living worms was calculated after 12 to 16 h of recovery. For pharmacological assays, starting at hatching, worms were grown on NGM plates containing 10 mM EGTA or 10 µM dantrolene, and survival after heat stroke was tested at the young adult stage. For time-course analysis of heat-stroke survivors either without or after heat preconditioning, animals were scored over time for free locomotion or movement of the head or tail region of the body after gentle tapping of the plate. Animals positive for any of the above criteria were considered as alive.

**$Ca^{2+}$ monitoring.** For intracellular $Ca^{2+}$ monitoring experiments, transgenic animals expressing the $Ca^{2+}$ reporter GCaMP2.0 in the six touch receptor neurons were examined under a Zeiss AxioImager Z2 epifluorescence microscope. For heat-stroke-induced neurodegeneration, heat-treated and preconditioned animals were monitored 3 h after the corresponding treatments. For necrosis triggered by the toxic MEC-4(d) channel, early hatched L1 larvae were monitored. Only neurons of very initial stages of degeneration (based on morphological features using DIC microscopy) were used for analysis, as the expression of GCaMP2.0 ceases during later stages of neurodegeneration. Images of neuron cell bodies were acquired under the same exposure. The emission intensity of GCaMP2.0 was calculated by using the ImageJ software (http://rsb.info.nih.gov/ij/).

**Electron microscopy.** High-pressure freezing (HPF) was carried out as described previously[54] and 50 nm sections were analysed. Micrographs were taken with a 1,024 × 1,024-pixel charge-coupled device detector (Proscan CCD HSS 512/1024; Proscan Electronic Systems) in an electron micrograph (EM902A; Carl Zeiss) operated in the bright field mode.

**Messenger RNA quantification.** To quantify *hsp-16.1*, *hsp-16.41*, *hsp-70*, *dnj-19* and *pmr-1* mRNA levels, total RNA was extracted using the TRIzol reagent (Invitrogen). The following sets of primers were used respectively: 5′-GGCT CTCCATCTGAATCTTCTGAG-3′ and 5′-TTCAAATCTTCTGGCTTGAACT GC-3′, 5′-TCATGCTCCGTTCTCCATATTC-3′ and 5′-ATTCATCATTTAC AATCTCCCC-3′, 5′-AGCTCTGTGCTGATCTTTTCCG-3′ and 5′-ATGGAG CAGTTGAGGTCCTTCC-3′, 5′-AGATGTTATCAAGCCAGGAGTC-3′ and 5′-AGCAGCTTTTCAGAACGGCAT-3′, 5′-ACGTGGAGAGAGTATGCAA TC-3′ and 5′-TACCGAGGGATTGACCAATGC-3′. Results were normalized to genomic DNA using the following primers specific for *ama-1*: 5′-CCT ACCTACACTCCAAGTCCATCG-3′ or 5′GGTGAAGCTGGCGAATACGT TG-3′. For cDNA synthesis, mRNA was reverse transcribed using the iScript cDNA Synthesis Kit (BioRad).Quantitative PCR was performed in triplicate using the Bio-Rad CFX96 Real-Time PCR system (BioRad).

**Neuronal cultures.** ESC-derived neurons were obtained from the differentiation of J1 ESCs following previously described protocols[55]. For primary cortical cultures, the cortex was dissected from E16 mouse embryos in PBS (137 mM NaCl, 2.7 mM KCl, 8 mM $Na_2HPO_4$ and 1.46 mM $KH_2PO_4$) containing glucose (0.2%) and BSA (0.1%), and was trypsinized for 15 min in 0.5% trypsin solution at 37 °C, followed by mechanical dissociation with a glass capillary. Neurons were plated at an initial density of 200,000 cells per $cm^2$ and cultured in neurobasal medium supplemented with 2% B27, 200 µM glutamine, 5 µg µl$^{-1}$ penicillin and 12.5 µg µl$^{-1}$ streptomycin. For some experiments, ESC-derived and cortical neurons were infected with lentiviruses 24 h after plating. For *Pmr1* knockdown, functionally validated shRNAs against PMR1 (Invitrogen, previously described in ref. 56) were electroporated into ESCs. ESCs stably expressing the shRNAs were selected using 240 µg µl$^{-1}$ G418, and single clones were isolated and differentiated into neurons as described earlier[55].

**Mammalian neuron heat stroke and preconditioning assays.** Preconditioning of neuronal cultures was carried out by placing them at 39 °C for 1 h in a $CO_2$ incubator, and cultures were placed back to 37 °C for 1 h to recover before proceeding to heat stroke. Heat stroke was simulated by exposing the neuronal cultures to 42 °C for 20 min in a $CO_2$ incubator. For the duration of the assays, the level of $CO_2$ was kept constant at 5%, similar to normal culturing conditions. After heat stroke, cells were returned to 37 °C for 15 min to recover and during this period propidium iodide (3 µg ml$^{-1}$) was added to the medium to stain necrotic neurons.

**Production of lentiviruses.** A modified LenLox3.7 plasmid (pLV) containing the human synapsin (hSYN) promoter[57] was used as a control. *Cryaa* cDNA was cloned after the hSYN promoter of pLV using *Bam*HI and *Not*I sites. Lentiviruses were produced in HEK293 cells triple-transfected transiently with pVSV-G and pΔ8.1 vectors (gift from G. Sourvinos) and with either the empty pLV-hSYN or pLV-hSYN-Cryaa plasmids. The supernatant containing the viral particles was collected 2 to 3 days post transfection and titre was determined by serial dilutions.

***Pmr1* knockdown.** For *Pmr1* downregulation, shRNAs against mouse *Pmr1* were designed by modifying validated oligonucleotides previously used to downregulate the highly homologous human *Pmr1* (described in ref. 56). The resulting oligonucleotides that were used in our study are the following: 5′-CGTC AAGAAGTAACATCGCCTTCA-3′ and 5′-CAGTGGATAAAGATGTCATT CGAAA-3′. An short interfering RNA (siRNA) expression vector containing a neomycin resistance cassette (Genscript, catalogue no. SD1100) was used to express the shRNAs under the H1 promoter. The shRNA inserts were built using the above oligonucleotides in a sense-loop-antisense-termination sequence flanked by *Bam*HI and *Hind*III sites on the 5′ and 3′ ends, respectively. The loop sequence used was TTCAAGAGA and the termination signal TTTTTT. Therefore, the sequences of the shRNA inserts are as follows: insert 1: 5′-GGATCCCCGTCAAGAAGTAACATCGCCTTCATTCAAGAGATGAAGG CGATGTTACTTCTTGACGTTTTTTCCAAAGCTT-3′, and insert 2: 5′-GGA TCCCCAGTGGATAAAGATGTCATTCGAAATTCAAGAGATTTCGAATGA CATCTTTATCCACTGTTTTTTCCAAACGTT-3′. The shRNA inserts were cloned into the vector using *Bam*HI and *Hind*III sites, also present as unique sites in the vector. Plasmids containing the shRNAs were linearized using *Not*I, phenol-chloroform extracted and twice precipitated with ethanol, and electroporated into ESCs. Electroporation was carried out using an ECM830 square wave BTX electroporator (set at 320 V, 1 pulse, 99 µs). Electroporated ESCs were plated on neomycin-resistant feeders and were treated with 240 µg ml$^{-1}$ G418, starting

24 h after electroporation and for 7 days. Neomycin-resistant ESCs grew as separate colonies on the feeders. Single ESC colonies were picked mechanically, each plated in a well of a 96-well plate containing feeders and expanded in the presence of G418. Thereafter, four colonies were further differentiated into neurons and levels of *Pmr1* were analysed by Western Blot analysis of lysates obtained from these neurons.

**Western blot analysis.** Cells were lysed in 500 mM Tris-HCl pH 7.2, containing 1 M NaCl, EDTA, Triton X-100, Na-deoxycholate, 10% SDS, supplemented with 1 mM DTT (dithiothreitol) and protease inhibitors (Roche) and placed for 20 min on ice followed by a 20-min centrifugation at 10,000*g*, at 4 °C. Supernatants were separated on an 8% acrylamide gel and transferred to a nitrocellulose membrane. After overnight blocking with 5% skimmed milk in TPBS (PBS with 0.1% Tween-20) at 4 °C, membranes were incubated overnight with primary antibodies prepared in blocking solution, at 4 °C. After several washes with TPBS, membranes were incubated for 1 h with secondary, horse radish peroxidase (HRP)-conjugated antibodies, at room temperature. After several washes with TPBS, membranes were incubated with enhanced chemiluminescence (ECL) substrate for 5 min (Thermo Scientific) and developed using the LAS-3000 imaging system. The primary antibodies used for Western Blot analysis were anti-PMR1 (gift of J. Vanoevelen and F. Wuytack, diluted at a ratio of 1:500) and anti-β-III tubulin (Covance, MMS-435P-250, diluted at a ratio of 1:5000).

**Immunocytochemistry.** Cells were fixed for 20 min at 37 °C in 4% paraformaldehyde (PFA). After several washes with PBS, cells were incubated in blocking solution (10% serum, 0.2% Triton-X in PBS) for 1 h at 25 °C and then overnight at 4 °C in blocking solution containing primary antibody. After several washes with PBS, cells were incubated with secondary antibody diluted in PBS. The nuclear dye Hoechst 33342 (Thermo Scientific) was also added during this incubation period. The following primary antibodies were used: anti-β-III tubulin (Covance, MMS-435P-250, diluted at a ratio of 1:2000), anti-crystallin αA (Santa Cruz sc-22389, 1:500), anti-mannosidase II (gift of S. Mitrovic, diluted at a ratio of 1:2000) and anti-PMR1 (gift of J. Vanoevelen, diluted at a ratio of 1:500). For the co-labelling of CRYAA and PMR1, an antigen retrieval treatment was necessary. Briefly, cells were placed in 10 mM sodium citrate and microwaved for 30 s so that the solution came to boil. Subsequently, they were immediately placed on ice for 5 min. This boil–cold cycle was repeated two more times and then the citrate buffer was removed and cells were incubated in blocking solution and stained following the standard procedure described above. Images were acquired using the Zeiss LSM 710 confocal microscope.

**Statistical analysis.** The Prism software package (GraphPad Software) and the Microsoft Office 2003 Excel software package (Microsoft Corporation) were used to carry out statistical analyses. Mean values were compared using unpaired *t*-tests. For multiple comparisons, we used one- and two-way ANOVA, corrected by the post-hoc Bonferroni test. Information about *P* values and experiment specifics (*n*, statistical significance tests) for all main figures are provided in their respective figure legends.


51. Brenner, S. The genetics of Caenorhabditis elegans. *Genetics* **77,** 71–94 (1974).
52. Gitler, A. D. *et al.* The Parkinson's disease protein alpha-synuclein disrupts cellular Rab homeostasis. *Proc. Natl Acad. Sci. USA* **105,** 145–150 (2008).
53. Artal-Sanz, M., Samara, C., Syntichaki, P. & Tavernarakis, N. Lysosomal biogenesis and function is critical for necrotic cell death in Caenorhabditis elegans. *J. Cell Biol.* **173,** 231–239 (2006).
54. Rostaing, P., Weimer, R. M., Jorgensen, E. M., Triller, A. & Bessereau, J. L. Preservation of immunoreactivity and fine structure of adult C. elegans tissues using high-pressure freezing. *J. Histochem. Cytochem.* **52,** 1–12 (2004).
55. Bibel, M., Richter, J., Lacroix, E. & Barde, Y. A. Generation of a defined and uniform population of CNS progenitors and neurons from mouse embryonic stem cells. *Nature Protocols* **2,** 1034–1043 (2007).
56. von Blume, J. *et al.* ADF/cofilin regulates secretory cargo sorting at the TGN via the Ca2+ ATPase SPCA1. *Dev. Cell* **20,** 652–662 (2011).
57. Gascón, S., Paez-Gomez, J. A., Diaz-Guerra, M., Scheiffele, P. & Scholl, F. G. Dual-promoter lentiviral vectors for constitutive and regulated gene expression in neurons. *J. Neurosci. Methods* **168,** 104–112 (2008).